Original paper

Evaluation of ^{101}Rh as a brachytherapy source

Delaram Pakravan, MSc[1], Mahdi Ghorbani, PhD[2], Ali Soleimani Meigooni, PhD[3,4]

[1]Department of Physics, Faculty of Basic Sciences, Ahvaz Branch, Islamic Azad University, Ahvaz, Iran, [2]Medical Physics Research Center, Faculty of Medicine, Mashhad University of Medical Sciences, Mashhad, Iran, [3]Comprehensive Cancer Centers of Nevada, Las Vegas, Nevada, USA, [4]School of Allied Health Science, University of Nevada Las Vegas (UNLV), Las Vegas, Nevada, USA

Abstract

Purpose: Recently a number of hypothetical sources have been proposed and evaluated for use in brachytherapy. In the present study, a hypothetical ^{101}Rh source with mean photon energy of 121.5 keV and half-life of 3.3 years, has been evaluated as an alternative to the existing high-dose-rate (HDR) sources. Dosimetric characteristics of this source model have been determined following the recommendation of the Task Group 43 (TG-43) of the American Association of the Physicist in Medicine (AAPM), and the results are compared with the published data for ^{57}Co source and Flexisource ^{192}Ir sources with similar geometries.

Material and methods: MCNPX Monte Carlo code was used for simulation of the ^{101}Rh hypothetical HDR source design. Geometric design of this hypothetical source was considered to be similar to that of Flexisource ^{192}Ir source. Task group No. 43 dosimetric parameters, including air kerma strength per mCi, dose rate constant, radial dose function, and two dimensional (2D) anisotropy functions were calculated for the ^{101}Rh source through simulations.

Results: Air kerma strength per activity and dose rate constant for the hypothetical ^{101}Rh source were 1.09 ± 0.01 U/mCi and 1.18 ± 0.08 cGy/(h.U), respectively. At distances beyond 1.0 cm in phantom, radial dose function for the hypothetical ^{101}Rh source is higher than that of ^{192}Ir. It has also similar 2D anisotropy functions to the Flexisource ^{192}Ir source.

Conclusions: ^{101}Rh is proposed as an alternative to the existing HDR sources for use in brachytherapy. This source provides medium energy photons, relatively long half-life, higher dose rate constant and radial dose function, and similar 2D anisotropy function to the Flexisource ^{192}Ir HDR source design. The longer half-life of the source reduces the frequency of the source exchange for the clinical environment.

J Contemp Brachytherapy 2015; 7, 2: 171-180
DOI: 10.5114/jcb.2015.50662

Key words: brachytherapy, hypothetical source, ^{101}Rh, TG-43 dosimetric parameters.

Purpose

Brachytherapy procedures have been used for treatment of cancer patients by radiation emitted from small encapsulated sources. In this treatment modality, the sources are placed directly into the tumor or adjacent to the treatment volume. The common radionuclides of brachytherapy sources are ^{60}Co, ^{137}Cs, ^{192}Ir, ^{198}Au, ^{125}I, and ^{103}Pd [1-4]. ^{192}Ir can be accounted as the most commonly radionuclide used for both low-dose-rate (LDR) and high-dose-rate (HDR) brachytherapy sources. Recently, new radionuclides have been considered as alternatives to the above noted sources in brachytherapy treatments. These sources include ^{131}Cs, ^{169}Yb, ^{57}Co, ^{153}Gd, and ^{170}Tm [5-12]. ^{131}Cs was proposed as low dose rate seeds [5]. Radial dose function of ^{131}Cs is similar to those of ^{125}I sources but it has radiobiological advantages in permanent brachytherapy implants over other sources due to its shorter half-life [5,6]. ^{169}Yb and ^{170}Tm with average energies of 93 keV and 66.39 keV and half-lives of 32 days and 128.6 days, respectively, are interesting for use as HDR brachytherapy sources [7-10]. ^{57}Co emits photons with energies of 122 and 136 keV and half-life of 272 days [11]. Two dimensional (2D) anisotropy function of ^{57}Co is comparable to that of ^{192}Ir and its radial dose function has an increasing trend in some distances, which could lead to larger dose to deeper tissue [11]. ^{153}Gd radionuclide with average energy of 60.9 keV was proposed as a low dose rate or pulsed dose rate brachytherapy source [12]. Enger *et al.* have shown that this source can be used for interstitial brachytherapy with rotating shield in needle [12]. These new radionuclides, despite having average energies lower than ^{192}Ir, have high enough energy to minimize photoelectric interactions in soft tissue. With these sources, a smaller shielding is required relative to ^{192}Ir sources. The drawbacks of some of the new hypothetical isotopes can be related to their short half-life, beta contamination, and bremsstrahlung contributions. For example, the yield of the photons emission of ^{170}Tm

Address for correspondence: Delaram Pakravan, MSc, Department of Physics, Ahvaz Branch, Islamic Azad University, Golestan Blvd., Farhang Shahr, Ahvaz, Iran, PO Box: 61349-37333, phone: +986113348420-24, fax: +986113329200, e-mail: pakravan@iauahvaz.ac.ir

Received: 23.08.2014
Accepted: 15.02.2015
Published: 30.04.2015

Table 1. The photon energy spectrum emitted by ^{101}Rh radionuclide [15]

Assignment	Energy (keV)	Prevalence (%)
$\gamma_1(^{101}Ru)$	110.94	0.04415
$\gamma_2(^{101}Ru)$	127.227	68.07
$\gamma_3(^{101}Ru)$	184.1	0.0591
$\gamma_4(^{101}Ru)$	197.99	73
$\gamma_5(^{101}Ru)$	295.01	0.59518
$\gamma_6(^{101}Ru)$	325.23	11.8311
$\gamma_7(^{101}Ru)$	422.1	0.19911
Ru L_l	2.253	0.10318
Ru L_η	2.382	0.0477
Ru $L_{\alpha 2}$	2.554	0.274
Ru $L_{\alpha 1}$	2.558	2.44
Ru $L_{\beta 1}$	2.683	1.1818
Ru $L_{\beta 4}$	2.741	0.09123
Ru $L_{\beta 6}$	2.763	0.015624
Ru $L_{\beta 3}$	2.763	0.133
Ru $L_{\beta 2}$	2.836	0.224
Ru $L_{\gamma 1}$	2.965	0.08613
Ru $L_{\gamma 2}$	3.181	0.0154
Ru $L_{\gamma 3}$	3.181	0.0277
Ru $K_{\alpha 3}$	18.893	0.000653
Ru $K_{\alpha 2}$	19.15	22.88
Ru $K_{\alpha 1}$	19.279	43.315
Ru $K_{\beta 3}$	21.634	3.5512
Ru $K_{\beta 1}$	21.657	6.8723
Ru $K_{\beta 5}$	21.836	0.04112
Ru $K_{\beta 2}$	22.074	1.615
Ru $K_{\beta 4}$	22.115	0.33616

is lower than the yield its electron emission (6 photons per 100 electrons emitted).

The energy of the photon emission and half-life of Rhodium-101 (^{101}Rh) make this radionuclide a possible candidate as a brachytherapy source. ^{101}Rh can be produced by nuclear reactions of ^{101}Ru(d, 2n)^{101}Rh or ^{102}Ru (d, 3n)^{101}Rh in a cyclotron. Prototype radionuclides have been produced at the isochronous cyclotron at the HISKP (Helmholtz-Instituts für Strahlen-und Kernphysik) of the University of Bonn (Germany) [13]. A natural ruthenium foil (with 20 mm^2 cross-section and 0.3 mm thickness) was applied as target, which included ^{101}Ru and ^{102}Ru isotopes. A number of typical factors used in this nuclear reaction are: 1) deuteron energy: 27 MeV; cross section: 1000 mbarn; deuteron beam intensity: 1 μA; 2) irradiation time: 2 days; ^{101}Rh activity after cool-down period of 43 days: 1 MBq [13]. Advantages of ^{101}Rh over the existing ^{192}Ir may be due to its relatively longer half-life of 3.3 years, higher specific activity of 397 TBq/g, and lower mean photon energy of 121.5 keV as shown in Tables 1 and 2. These adequate physical characteristics made this radioisotope interesting for this project for evaluation as a possible alternative for the HDR brachytherapy source. The purpose of this work is to evaluate the dosimetric parameters of a hypothetical ^{101}Rh source using task group No. 43 (TG-43) recommendations and verify if it would be a potential HDR brachytherapy source.

Material and methods

Design for the hypothetical ^{101}Rh source

In this project, the geometric structure of the hypothetical ^{101}Rh source was designed to be similar to the Flexisource ^{192}Ir HDR source [14], just for the ease of the comparison of the dosimetric parameters between the two sources. The design and dimensions of ^{101}Rh source is shown in Figure 1. The active core of the source is a pure ^{101}Rh cylinder (density of 12.41 g/cm^3) with an active length of 3.5 mm and an active diameter of 0.6 mm. The active core is covered by a 304 stainless steel capsule (composition by weight – Fe: 67.92%, Cr: 19%, Ni: 10%, Mn: 2%, Si: 1% and C: 0.08%; density: 8.0 g/cm^3). The outer dimensions of the source are 0.85 mm in diameter and 4.6 mm in total length. The 304 stainless steel cable (density of 8.0 g/cm^3) has been considered as a cylinder with a length of 5 mm and a diam-

Table 2. Characteristics of the ^{57}Co, ^{101}Rh and ^{192}Ir sources

	^{57}Co	^{101}Rh	^{192}Ir
Specific activity (TBq/g)	312	397	341
Half-life	272 days	3.3 years	74 days
Photon energy (keV)	122, 136	121.5 (average)	360 (average)
Yield (photons/disintegration)	1.61	2.37	2.36
Air kerma strength per activity (U/mCi)	0.46	1.09 ± 0.01	3.62
Dose rate constant (cGy/(hU))	1.215	1.18 ± 0.08	1.114
Half-value layer in lead (mm)	0.298	0.0331	2.97

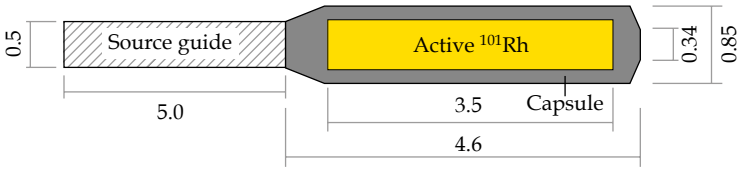

Fig. 1. Geometric design of the ^{101}Rh hypothetical source (all dimensions are in millimeters). This figure is not to scale

eter of 0.5 mm. The energy spectrum of the ^{101}Rh photons considered in this study is listed in Table 1 [15].

Calculation of TG-43 dosimetric parameters

Based on updated TG-43 formalism [2], dose rate at a point is calculated from the following formula:

$$\dot{D}(r,\theta) = S_K \Lambda \frac{G(r,\theta)}{G(r_0,\theta_0)} g(\mathrm{r})\, F(r,\theta) \quad (1)$$

In the above formula, S_K, Λ, $G(r,\theta)$, $g(r)$ and $F(r,\theta)$ present air kerma strength, dose rate constant, geometry function, radial dose function, and 2D anisotropy function, respectively. The MCNPX Monte Carlo (MC) code (version 2.4.0) [16] was used for obtaining dosimetric parameters of the new source design. In the calculations, only photons emitted by the ^{101}Rh were defined in the source definition card. It was assumed that the beta particles emitted by the source (ranging 118.78-541 keV with the most probable energy of 215.77) are absorbed by the encapsulation of source, therefore they were ignored.

For estimation of air kerma strength, a torus with a minor diameter of 0.5 mm and major radii of 20 cm was defined on the transverse plane of the hypothetical source. F6 tally, which is a commonly used tally in MCNP simulations, was used for these calculations and the results were obtained in terms of kerma of the source in MeV/(g.photon). This torus is composed of air and the surrounding phantom material is composed of vacuum. Air kerma strength then was calculated from the air kerma strength formula presented in the updated TG-43 formalism using the kerma value and the corresponding units and other conversion factors (such as eV to joule, grams to kilograms, photon yields, etc.).

For determination of dose rate constant, the hypothetical source was positioned at the center of a spherical water phantom with radius of 50 cm in the simulations. A torus with 0.5 mm minor diameter and major radii of 1.0 cm was defined on the transverse plane and *F8 tally was calculated. This torus was also composed of water. Using *F8 tally (in terms of MeV) in MCNP it is feasible to score the absorbed energy inside a tally cell. Therefore, dose rate is output of *F8 tally divided by the mass of the torus considering the units for conversion factors (for example, eV to joule, grams to kilograms, yields, etc.). Dose rate constant then was obtained as the dose rate divided by the air kerma strength.

As an example for conversion of the MC output (for *F8 tally divided per mass in terms of: MeV/g per photon) to absorbed dose rate in units of cGy/(h.mCi) the following formula can be used:

Dose rate (cGy/h) = MC output (MeV/g per photon) × × 10^6 (eV/MeV) × 1.602 × 10^{-19} (J/eV) × 10^3 (g/kg) × × 1.0 mCi × 10^{-3} (Ci/mCi) × 3.7 × 10^{10} (Bq/Ci) × 1 (dis/s per Bq) × photon yield of ^{101}Rh (photons/dis) × 100 (cGy/Gy) × 3600 (s/h) (2)

with this regard, the value of photon yield of the ^{101}Rh radionuclide is equal to 2.37 photons/dis. This value can be obtained from summation and normalization of the prevalences listed in Table 1. The activity of ^{101}Rh source, used in this conversion was equal to 1.0 mCi.

In order to calculate radial dose function of the new source design, a spherical water phantom with 50 cm radius was defined with the source located at the center of the phantom. Torus voxels were considered at distances of 0.1-15.0 cm on the transverse plane of the source in the phantom. The thicknesses of the tori were 0.4 mm at distances up to 1.0 cm, and 1.0 mm for other distances up to 15.0 cm. The outputs of *F4 tally was used for calculation of dose rate at various radial distances. To have an acceptable level of uncertainty, this type of tally was used to speed up the calculations in the MCNP simulations. A line-source approximation was applied in calculation of two dimensional geometry functions. Finally, radial dose function was calculated from dose rate and geometry function values at various distances.

For calculation of 2D anisotropy function, the same phantom (i.e. spherical water phantom with 50 cm radius) was defined as that described in calculation of radial dose function. For these simulations, the calculation points were located on a circular path around the source with the same radial distances, and different polar angles, ranging from 0° to 180° angles at 5 degrees intervals. These points were divided into two groups, those that were along the longitudinal axis of the source, and those that were off the longitudinal axis. Spherical voxels with 0.1 cm diameter were utilized to score the dose on the longitudinal axis of the source. For the other points, tori with minor diameter of 0.4 mm were defined at radial distances of 0.5 cm and 1.0 cm. The minor diamaters of these tori were 1 mm for larger distances (larger than 1.0 cm, up to 15.0 cm). The reason for different tally voxel sizes at various distances is due to the presence of steep dose gradient as a function of distance from the source, which is an inherent effect in brachytherapy. Therefore, using larger voxel size at shorter distances may introduce artifacts in the calculations by volume-averaging. The outputs of *F4 was used for calculation of 2D anisotropy functions. From the selected tallies at various distances, the 2D anisotropy function values were calculated for distances ranging between 0.5-15.0 cm and for angles be-

tween 0° to 180° with 5.0 degrees intervals. In calculation of TG-43 parameters, toroidal cells were used to comply with the cylindrical symmetry of the dose distribution. An attempt was also made to use toroid cells not having large dimensions at various reference directions to avoid volume-averaging artifacts. As an example, for calculation of anisotropy function at 2.0 cm distance and 30° angle, a torus with minor diameter of 1 mm at horizontal and vertical directions was utilized. It should be noticed that in these calculations, the source delivery cable is coincident on the angle of 180 degrees.

Table 3. Radial dose function for ^{101}Rh hypothetical source

Radial distance r (cm)	$g_L(r)$
0.1	0.944
0.2	0.953
0.3	0.961
0.4	0.966
0.5	0.968
0.6	0.973
0.7	0.978
0.8	0.985
0.9	0.995
1.0	1.000
1.5	1.021
2.0	1.045
2.5	1.062
3.0	1.080
3.5	1.099
4.0	1.118
4.5	1.126
5.0	1.139
5.5	1.147
6.0	1.154
6.5	1.161
7.0	1.162
7.5	1.164
8.0	1.158
8.5	1.163
9.0	1.153
9.5	1.149
10.0	1.139
12.0	1.103
15.0	1.013

In all calculations, the energy cut off of 1 keV was defined for photons and electrons. For calculation of TG-43 dosimetric parameters, except for 2D anisotropy function, the input files were run for 2.5×10^7 particles. For calculation of 2D anisotropy function, in order to reduce the calculation uncertainties at larger distances from the source, the input file was run for 10^8 photons. The maximum type A errors or statistical uncertainties in Monte Carlo calculations for air kerma strength, dose rate constant and radial dose function over all the evaluated distances were 0.3%, 3.32% and 0.44%, respectively. The reason for having larger uncertainty in dose rate constant than the other two parameters was due to the use of *F8 tally in this case compared to F6 or *F4 tallies for the others. For similar particle scoring numbers, using *F8 tally in MCNP normally incorporates to larger uncertainty compared to the other tallies. The maximum type A uncertainty in calculation of 2D anisotropy function was 4.42%. It should be noted that these values are type A uncertainties, by having ignored type B uncertainties and with a coverage factor (k) of 2.0, the expanded uncertainties (U; $U = ku_c$, in which u_c is the combined uncertainty) will be twice these values. A coverage factor of 2.0 corresponds to 95% confidence level. With 95% confidence level, the true value is in the "calculated value – 2U" – "calculated value + 2U" interval with the probability of 0.95. The input programs were run using a personal computer having 64-bit Windows 7.0 operating system, 3.20 GHz Intel (R) Core i7 CPU, and 2.00 GB RAM. With this computer, the running time for the air kerma strength, dose rate constant, radial dose function, anisotropy function, with the aforementioned numbers of particles histories, was 5.25 h, 24.75 h, 25.50 h, and 134.25 h, respectively. Finally, the TG-43 dosimetric parameters of the hypothetical ^{101}Rh source were compared with the data for another hypothetical ^{57}Co source [17] and Flexisource ^{192}Ir source [14].

Results

Air kerma strength per activity and dose rate constant values for the hypothetical ^{101}Rh source were obtained, and found to be 1.09 ± 0.01 U/mCi and 1.18 ± 0.08 cGy/(hU), respectively. The errors in these values are reported with a coverage factor of 2σ. A comparison of other characteristics of these three sources is shown in Table 2. These characteristics include specific activity, half-life, average photons energy, etc. It can be noticed that the specific activity was calculated theoretically from: $S = (\lambda N_A)/M$.

Radial dose function of the hypothetical ^{101}Rh source as a function of radial distance is shown in Table 3. 2D anisotropy function values of the hypothetical ^{101}Rh as a function of radial distance and polar angles were listed in Table 4.

A comparison of the radial dose function of the hypothetical ^{101}Rh source with the published data for the hypothetical ^{57}Co source, and Flexisource ^{192}Ir source is shown in Figure 2. Moreover, Figure 3 shows the comparison between the 2D anisotropy function of the hypothet-

Table 4. 2D anisotropy function for [101]Rh hypothetical source

θ (degree)	Distance r (cm)								
	0.5	1.0	3.0	4.0	5.0	7.0	10.0	12.0	15.0
0	–	0.681	0.738	0.775	0.795	0.847	0.892	0.903	0.909
5	0.709	0.708	0.770	0.798	0.818	0.843	0.899	0.869	0.922
10	0.756	0.751	0.814	0.835	0.845	0.862	0.894	0.910	0.918
15	0.812	0.812	0.860	0.873	0.884	0.902	0.912	0.923	0.930
20	0.862	0.859	0.893	0.900	0.909	0.920	0.933	0.934	0.945
25	0.896	0.892	0.918	0.920	0.922	0.927	0.947	0.939	0.958
30	0.917	0.915	0.936	0.941	0.941	0.941	0.957	0.945	0.959
35	0.940	0.936	0.948	0.946	0.945	0.956	0.964	0.964	0.967
40	0.955	0.951	0.963	0.963	0.960	0.967	0.973	0.968	0.975
45	0.966	0.963	0.973	0.974	0.967	0.975	0.983	0.974	0.985
50	0.976	0.972	0.982	0.981	0.979	0.981	0.988	0.979	0.980
55	0.984	0.976	0.979	0.981	0.979	0.977	0.989	0.985	0.987
60	0.989	0.984	0.993	0.989	0.986	0.982	0.994	0.984	0.993
65	0.992	0.988	0.994	0.996	0.991	0.987	0.989	0.990	0.994
70	0.997	0.989	0.997	0.995	0.994	0.995	1.001	0.990	0.995
75	0.999	0.994	1.000	0.996	0.995	0.991	1.000	0.993	0.997
80	1.004	0.995	1.000	0.998	0.997	0.994	1.003	0.998	1.001
85	1.001	0.991	1.000	0.998	0.995	0.991	1.002	0.993	0.995
90	1.000	1.000	1.000	1.000	1.000	1.000	1.000	1.000	1.000
95	1.005	0.997	0.997	0.997	0.993	1.001	1.004	0.991	0.996
100	1.001	0.994	1.003	1.000	1.000	0.994	1.004	0.995	0.998
105	0.998	0.993	0.998	0.997	0.996	0.992	0.995	0.992	1.001
110	0.996	0.988	0.997	0.996	0.992	0.993	1.003	0.991	0.997
115	0.994	0.988	0.993	0.994	0.991	0.993	0.996	0.985	0.995
120	0.989	0.979	0.989	0.990	0.988	0.992	0.992	0.988	0.992
125	0.981	0.975	0.987	0.988	0.985	0.987	0.991	0.976	0.986
130	0.975	0.970	0.978	0.978	0.977	0.972	0.989	0.973	0.981
135	0.967	0.962	0.970	0.971	0.969	0.970	0.982	0.981	0.978
140	0.955	0.947	0.961	0.959	0.956	0.963	0.972	0.967	0.972
145	0.935	0.928	0.949	0.948	0.949	0.952	0.960	0.955	0.963
150	0.924	0.921	0.928	0.939	0.940	0.945	0.955	0.950	0.964
155	0.897	0.889	0.916	0.916	0.923	0.935	0.949	0.952	0.957
160	0.863	0.858	0.896	0.900	0.910	0.919	0.936	0.933	0.953
165	0.821	0.816	0.862	0.874	0.880	0.903	0.918	0.921	0.954
170	0.760	0.761	0.808	0.827	0.836	0.864	0.897	0.888	0.900
175	–	0.659	0.746	0.767	0.781	0.828	0.848	0.891	0.901
180	–	0.509	0.635	0.678	0.720	0.763	0.820	0.834	0.869

ical ^{101}Rh source and the values from hypothetical ^{57}Co source and Flexisource ^{192}Ir source, at the distances of 0.5, 1.0, 5.0, and 10.0 cm from the source. The data presented in Figures 2 and 3 for the hypothetical ^{57}Co source was obtained via personal communication [17]. The data for the Flexisource ^{192}Ir source in these figures were extracted from the data reported by Granero *et al*. [14].

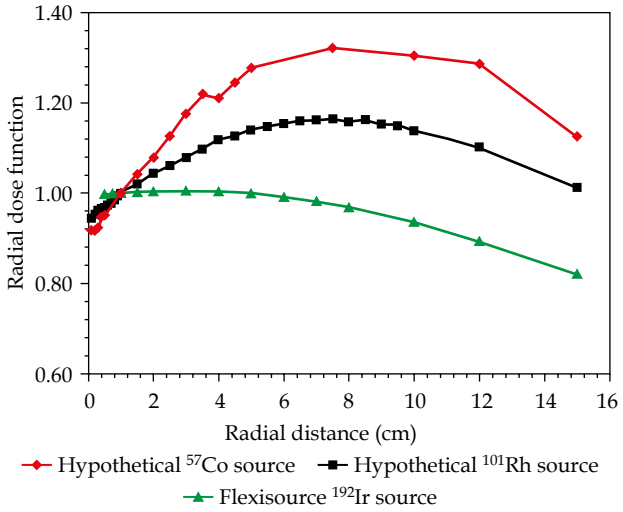

Fig. 2. A comparison of the radial dose function for the hypothetical ^{101}Rh source, hypothetical ^{57}Co source and Flexisource ^{192}Ir source

Discussion

Dosimetric comparison with other radionuclides

In the present study, TG-43 dosimetric parameters of a hypothetical ^{101}Rh source were calculated and compared with those of a hypothetical ^{57}Co and a commercially available Flexisource ^{192}Ir sources. Based on the data in Table 2, air kerma strength per mCi activity for the hypothetical ^{101}Rh source is higher (factor of 2.37) than that of the hypothetical ^{57}Co source and less (factor of 3.32) than that of ^{192}Ir source. Since all the three sources have the same geometrical structure, this effect is due to the differences in yield and specific activities, energy spectra of photons emitted from the radionuclides and self-absorptions inside the active cores. Higher air kerma strength per mCi is an advantage for ^{192}Ir brachytherapy source over ^{101}Rh. However, this source (^{101}Rh) has more than twice air kerma strength per mCi higher than that for ^{57}Co. Air kerma strength per mCi activity indicates the

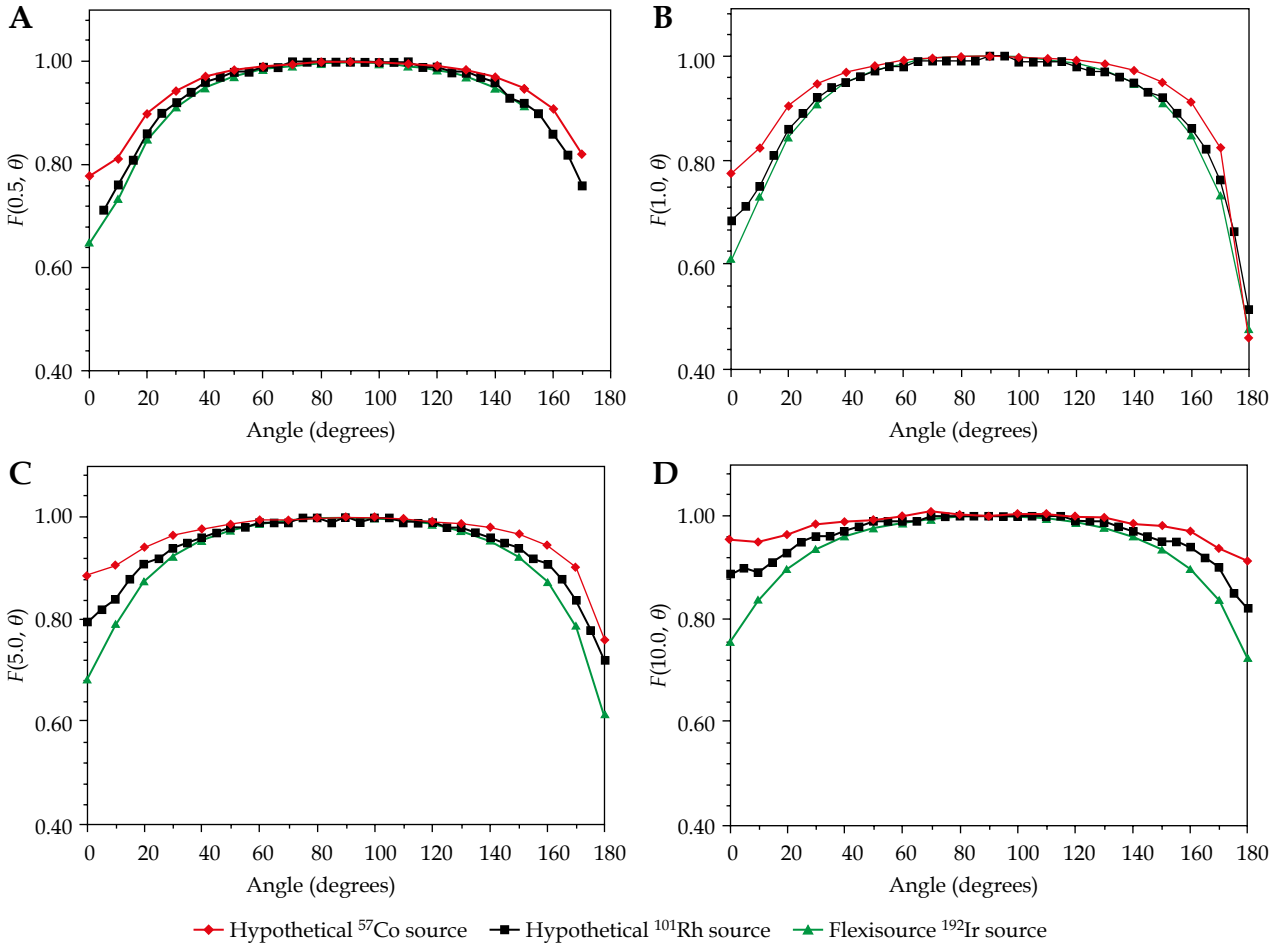

Fig. 3. A comparison of the 2D anisotropy function for the hypothetical ^{101}Rh source, hypothetical ^{57}Co source and Flexisource ^{192}Ir source at the distances of (A): 0.5 cm; (B): 1.0 cm; (C): 5.0 cm; (D): 10.0 cm from the source

level of self-absorption inside a source, and depends on the energy spectrum of a radionuclide and source design. On the other hand, dose rate constant of the hypothetical ^{101}Rh source is approximately the same as than those for ^{57}Co and ^{192}Ir sources. Therefore, it can be concluded that per U of air kerma strength, these sources can release the same dose rates at the reference distance (1.0 cm) from the source in water.

Based on the data presented in Figure 2, radial dose function for the hypothetical ^{101}Rh source is larger than the values for ^{192}Ir source for distances greater than 1.0 cm. This comparison indicates that there would be a larger dose delivered to the tissues located at larger distances from the hypothetical ^{101}Rh source than the ^{192}Ir source. For example, at a distance of 8.0 cm, the radial dose functions of the ^{101}Rh and ^{192}Ir sources are 1.16 and 0.96, respectively. Therefore, at this distance, ^{101}Rh delivers approximately 21% larger dose than ^{192}Ir source. This is an excellent advantage for brachytherapy treatment of many different cancer patients, such as cervical or deep seated vaginal cancer. Moreover, the skin sparing characteristics of the ^{101}Rh source may become superior to the ^{192}Ir sources for some treatments such as the breast cancer with AccuBoost system [18]. Interestingly, this graph indicates that the ^{57}Co source delivers larger dose than both ^{101}Rh and ^{192}Ir sources, which can be accounted as an advantage for this source.

Figure 3 shows that, except at very small angles (< 20 degrees), the 2D anisotropy function data of ^{101}Rh very similar to the ^{192}Ir and ^{57}Co data for all distances. 2D anisotropy function explains the non-isotropic feature of dose distribution around the source due to self-absorption within the source and distribution of the activity with a linear pattern.

It should be clear that the present results of TG-43 parameters for the ^{101}Rh source are only valid for the geometry design that is defined in this study and they cannot be used for the clinical purposes. Therefore, the dose distribution and the TG-43 parameters will change by variation in the source design for the hypothetical ^{101}Rh sources. In other words, the results of this work, especially anisotropy, depend on the structural details of the source design. Moreover, anisotropy cannot be used as a criterion for advocating the use of a new radionuclide for brachytherapy. There are cases, in which highly anisotropic sources can be used effectively, provided their anisotropy function is accurately known. This leaves air kerma strength, dose rate constant, and radial dose function as TG-43 quantities meaningful for the evaluation of a candidate radionuclide for brachytherapy. Their appropriateness, however, should be assessed in the context of a specific application. As a sample, the study by Lymperopoulou *et al*. [19] compares ^{169}Yb with ^{192}Ir for use as sources in prostate brachytherapy. The same evaluations can be performed for the ^{101}Rh radionuclide for application in prostate brachytherapy. In the following text, some aspects of use of this source in interstitial rotating shield brachytherapy (I-RSBT) are described.

Based on the data presented in Table 2, the energy of photons emitted by ^{101}Rh is on average lower than ^{192}Ir. Therefore, for medium energy photons emitted by ^{101}Rh, the required thickness of the shielding (with half-value layer of 0.0331 mm lead [20]) is much lower than that needed for protection against ^{192}Ir brachytherapy source (2.97 mm lead). It should be noticed that having compared only the average photon energies of these sources (Table 2), the HVL differences are not justified. Therefore, considering the energy spectra of the sources can be illuminating. The lower thickness for shielding requirement will reduce the costs of treatment room shielding for the ^{101}Rh source. Other advantages of ^{101}Rh are relatively long half-life of 3.3 years and high specific activity of 397 TBq/g. These suitable characteristics made ^{101}Rh radionuclide interesting for application as a brachytherapy source. On the other hand, air kerma strength per mCi activity of the ^{101}Rh source with the proposed geometry is lower than that of ^{192}Ir source. While this effect will depend on the geometries of these two sources with the assumed geometries, this can be an advantage of ^{192}Ir over ^{101}Rh. This is because that with the same and specific activities for these two sources, with ^{192}Ir the source strength will be higher and this is corresponded to a lower treatment time duration in a single treatment session.

As listed in Table 2, dose rate constant of the ^{101}Rh is 1.18 cGy/(h.U), which is approximately 6% larger than the ^{192}Ir value of 1.114. Therefore, the ^{101}Rh with the specified source design is able to deliver approximately 6% larger dose per air kerma strength than the ^{192}Ir source. The significance of this difference should be evaluated by considering the radiobiology of the treatment site.

Enger *et al*. [12] has reported a dose rate at 1.0 cm in water of 4.18×10^4 cGy/h for a VariSource ^{192}Ir source with activity of 370 GBq (i.e. equivalent to 10 Ci). This amounts to a dose rate per activity of 112.97 cGy/(h.GBq). Based on our Monte Carlo calculations, this quantity for the ^{101}Rh hypothetical source with a Flexisource design is equal to 35.29 cGy/(h.GBq). While this variable for ^{101}Rh source is lower than that of ^{192}Ir source, the source designs should be taken into account, since VariSource ^{192}Ir source has an active length of 10.0 mm but Flexisource design have a 3.5 mm one. This comparison was performed roughly for these two sources and a precise comparison should be performed with sources with the same geometries because self-absorption inside a source and encapsulation geometry and composition will affect the dose rate at 1.0 cm distance inside a water phantom. Generally, a lower dose rate per activity at 1.0 cm will need to higher activity or higher treatment time for a standard prescribed dose regime, and, therefore, for having a reasonable treatment time a multiple-source choice may be relevant. For having a higher activity, the production costs will be higher due to longer irradiation time needed for the target in a cyclotron or nuclear reactor. With this regard, a comparison more consistent with TG-43 formalism can be performed with comparison of dose rate constants of the sources. Since in dose rate constant, dose rate is normalized to air kerma strength (instead of activity in mCi) and having mCi to U conversion factors for the ^{192}Ir and ^{101}Rh sources is necessary to have a conversion from dose rate at 1.0 cm per activity to dose rate constant.

In a study by Lymperopoulou *et al*. [21], Monte Carlo simulation was utilized and ^{169}Yb was compared to ^{192}Ir

for breast HDR brachytherapy with multiple catheter implants. The results using dose volume histogram indicated that ^{169}Yb could be at least as effective as ^{192}Ir in delivering the same dose to the lung and with slightly less dose to the skin on breast. The finding implied that for the sources with intermediate photon energy such as ^{169}Yb, there is a need for the modification of calculation algorithms used in clinical treatment planning applied in particular brachytherapy practices. Lymperopoulou *et al*. [19] assumed a hypothetical ^{169}Yb source in evaluation of the use of this radionuclide for prostate HDR brachytherapy. ^{169}Yb proved to be at least equivalent to ^{192}Ir, independent to the prostate volume in the situation that the radiation scattering be overcompensated for absorption in intermediate energies and distances in prostate HDR brachytherapy. Having reviewed the methods used in the aforementioned studies, and the point that the ^{101}Rh source was evaluated only from TG-43 and general dosimetric specifications, it is recommended that this radionuclide be evaluated further in comparison with ^{192}Ir in brachytherapy applications for various cancers.

Production of ^{101}Rh

One may need to consider two other aspects of the ^{101}Rh source in application of this source in brachytherapy. One aspect is the costs of production of this radioisotope. Normally, radioisotopes are produced by a cyclotron or a nuclear reactor. It is mentioned in the introduction section that ^{101}Rh is produced by deuteron irradiation of isotopes of Ru. Theoretically, there are also other possible reactions for ^{101}Rh production. Some examples are: ^{103}Rh(n, 3n)^{101}Rh; ^{102}Pd(n, np)^{101}Rh and ^{102}Pd(n, d)^{101}Rh. ^{103}Rh and ^{102}Pd are natural isotopes of ruthenium and palladium, respectively. These reactions can be achieved by neutron irradiation of the target in a nuclear reactor. It should be noticed that these reactions require fast neutrons and are not accounted as fission reactions. The cross sections of these deuteron or neutron reactions are of importance when having enough activity of the ^{101}Rh product is aimed. Recently, a study was performed and it was disclosed that with 100 h cyclotron run time having 1 μA beam current, about 900 MBq of ^{101m}Rh can be produced [21]. In other words, the yield for production of ^{101m}Rh is 8.7 MBq/μAh [21]. ^{101m}Rh is metastable and decays to ^{101}Rh following gamma emission. A maximum beam current of 1 μA could be achieved in the experiments with Bonn cyclotron. However, cyclotrons with higher currents are also available. ISPRA cyclotron is an example having higher beam current. ^{101m}Rh decays to ^{101}Rh with a half-life of 4.34 days, and due to the short half-life of ^{101m}Rh and long half-life of ^{101}Rh, production of ^{101m}Rh with a cyclotron can be an alternative for achievement of ^{101}Rh [22]. As another pathway for production of ^{101}Rh, it was also reported that irradiation of ^{89}Y by ^{12}C can be proposed as a pathway to produce ^{101}Rh. ^{89}Y is the natural isotope of yttrium with 100% abundance. This reaction was obtained by ^{12}C beam with average energy of 49.5 MeV [23]. An issue, which could be considered with this process is the contamination of ^{101}Rh by other radionuclides and its influence on the TG-43 parameters. The cross section of ^{101}Rh as compared to those of ^{192}Ir is relevant in these considerations. ^{192}Ir is produced as a fission product in a nuclear reactor by irradiation of the target by thermal neutrons. Production of a radioisotope in a nuclear reactor result to lower production costs compared to a cyclotron. Although, due to lower energy photons emitted by ^{101}Rh relative to ^{192}Ir, the construction costs of shielding for treatment room may be lower, the production costs for ^{101}Rh source may be more than that of ^{192}Ir source. This issue should be considered before application of the ^{101}Rh radioisotope in brachytherapy.

Use of ^{101}Rh in interstitial rotating shield brachytherapy

I-RSBT method was evaluated for ^{153}Gd radioisotope in a study by Adams *et al*. [24]. In that study a novel needle, catheter and source system was presented for (I-RSBT) application in brachytherapy of prostate. Their justification for application of a shielded source and catheter system was their aim to reduce the dose received by urethra, rectum, and bladder. The reason for use of ^{153}Gd source instead of ^{125}I and ^{192}Ir sources was that ^{125}I sources has normally rapid dose fall-off in soft tissue and the thickness for shielding of ^{192}Ir sources would be large and cannot be fitted in catheters, which are normally used in prostate brachytherapy. Similar to ^{153}Gd, the same notifications can be considered for ^{101}Rh source. However, ^{101}Rh emits a number of relatively high energy photons albeit with lower prevalence (Table 1). The average photon energy and half-value layer (HVL) in lead for ^{101}Rh is much lower than that of ^{192}Ir. A comparison between the HVL for ^{153}Gd and ^{101}Rh may be interesting for use in I-RSBT. The HVL (in mm Pb) for ^{153}Gd and ^{101}Rh are 0.0783 and 0.0331, respectively [20]. It is evident that with ^{101}Rh a lower thickness of shielding is required in this method. However, a quantitative evaluation of shielding requirements for application in I-RSBT as a subject of further research in this field and will be interesting.

Limitations and suggestions for further research

The evaluations on the ^{101}Rh radionuclide could be accomplished simply using point source approximation that is time efficient but still meaningful with the purpose of only indication of an effect. A number of previous studies have used this approximation in their evaluations [25]. In a report on dose calculation in brachytherapy, it was proposed as a consideration for high energy photon emitting brachytherapy sources that modeling of sources using point source approximation is facilitated by averaging dose anisotropy over all angles. This method of calculation can be used in permanent prostate brachytherapy dose calculation, in which seed orientation is not distinguishable for clinical non-stranded application due to the large number of seed orientations [26]. Utilizing a point source could be easier and faster to perform but we preferred to execute a precise evaluation on this source similar to other articles on hypothetical sources by simulation of the source in its complete geometry [10-12].

Based on the AAPM and ESTRO report on high-energy sources [26], spherical phantom radius of 40 cm was recommended. The size of the spherical phantom used in this study is 50 cm and therefore the full scatter condition is obtained. This report also announced recommendations on maximum voxel sizes, which are being used for scoring the dosimetric variables to minimize the volume-averaging artifacts: (0.1 mm)^3 voxels for $r \leq 1$ cm; 0.5 × × 0.5 × 0.5 mm^3 voxels for 1 cm < $r \leq 5$ cm; 1 × 1 × 1 mm^3 voxels for 5 cm < $r \leq 10$ cm and 2 × 2 × 2 mm^3 voxels for 10 cm < $r \leq 20$ cm. In the present study, voxels are not cubic and are in the form of toroidal cells with 0.4 mm in thickness for $r < 1$ cm and with 1 mm thickness for the other distances. There are minor differences between our methodology for the thickness of the tally cells and those recommended by the AAPM and ESTRO report at close distances from the source, and this point should be noticed in the further methodologies.

The spectral data of ^{101}Rh radionuclide used in the simulations in this study (Table 1) were extracted from a database presented by Lund University [15]. On the other hand, a joint report by American Association of Physicists in Medicine (AAPM), and European Society for Therapeutic Radiology and Oncology **(**ESTRO) [26] recommends that National Nuclear Data Center (NNDC) data be used in application of brachytherapy sources, which are clinically related. NNDC includes three datasets for energy spectra of the ^{101}Rh radionuclide [26]. In a study by Rivard *et al*. [28], the influence of the choice of energy spectrum on kerma and dose distributions of three brachytherapy sources was evaluated. It was observed that there were water-kerma differences of about 2%, 2%, and 0.7% with various spectrum choices for ^{192}Ir, ^{125}I, and ^{103}Pd sources, respectively. Furthermore, the influence of photon spectrum on the dose rate constant and the radial dose function ranged from 0.1-2%. As a rough evaluation, the photon yields from the spectrum used in this study (Table 1) and the dataset No. 3 of NNDC [27] for ^{101}Rh are 2.3705 photons/dis. and 2.3670 photons/dis., respectively. The details are not presented herein but the spectrum used in the present study for the ^{101}Rh has more detailed energies than that announced by NNDC. While it is predicted that relatively the same results will be obtained with various choices of reference spectra for the hypothetical ^{101}Rh source, it is recommended that the spectrum from the NNDC website be used in the future studies on this source.

Treatment planning in brachytherapy has advancements starting from simple look-up tables up to computerized dose calculation algorithms. The current algorithms are based on the TG-43 formalism with recent advances in calculation of dose distributions for single sources. However, this formalism has limitations for calculation of patient dose. Various dose calculation algorithms are being developed based on: Monte Carlo methods, collapsed cone, etc. The scopes of current advancements in brachytherapy include: improved dose calculation tools, planning systems to account for heterogeneities, scattering conditions, radiobiology, and image guidance brachytherapy [29]. Following literature reports announcing the deficiencies involved in the approximations of conventional brachytherapy dosimetry, model-based dosimetry algorithms were incorporated in commercial brachytherapy treatment planning systems. The primary calculations of these algorithms are defined, having criteria established by the developers with the purpose of optimization of computation speed and accuracy. On the other hand, a basic realization of the limitations of these algorithms in commissioning step and their further evaluations compared to the conventional ones is necessary [30]. Task Group No. 186 provided guidance for early adopters of model-based dose calculation algorithms for brachytherapy users. Dose calculation accuracy in brachytherapy highly depends on the scatter conditions and photoelectric cross-sections relative to water. In some situations, differences between the TG-43 and model-based algorithms can lead to dose differences exceeding a factor of 10. Model-based dose calculation algorithms raise the major aspects, which are not addressed by current guidelines: dose sensitivity to the dose specification medium, dose calculation for the local medium in heterogeneous medium, and the dose in a small volume of water in heterogeneous medium. These issues are changed as patient-specific [31]. While in the present study ^{101}Rh was evaluated from only general and TG-43 dosimetric parameters, further evaluation of this source from the view of model-based dose calculation algorithms can be a subject of more complementary studies.

Conclusions

Advantages of ^{101}Rh to ^{192}Ir are having relatively longer half-life (3.3 years versus 74 days), higher specific activity (397 TBq/g versus 341 TBq/g)k, and very low half-value layer (0.0331 mm in lead versus 2.97 mm of lead). These adequate physical characteristics make this radionuclide interesting as a possible brachytherapy source. Air kerma strength per activity for hypothetical ^{101}Rh source is about twice than that of hypothetical ^{57}Co source and it has a dose rate constant comparable to hypothetical ^{57}Co and ^{192}Ir sources. Radial dose function for the ^{101}Rh hypothetical source is greater than that of ^{192}Ir source for distances greater than 1.0 cm. The 2D anisotropy function of ^{101}Rh is very similar to that of ^{192}Ir, which can be taken into account as another advantage of this new proposed source. With these suitable physical properties, ^{101}Rh could be considered as potential candidate in brachytherapy.

Acknowledgement

The authors gratefully acknowledge the Islamic Azad University (Ahvaz Branch) for financial support of this work.

Disclosure

Authors report no conflict of interest.

References

1. Nath R, Anderson LL, Luxton G et al. Dosimetry of interstitial brachytherapy sources: Recommendations of the AAPM

Radiation Therapy Committee Task Group No. 43. *Med Phys* 1995; 22: 209-234.
2. Rivard MJ, Coursey BM, Dewerd LA et al. Update of AAPM Task Group No. 43 Report: A revised AAPM protocol for brachytherapy dose calculation. *Med Phys* 2004; 31: 633-674.
3. Venselaar J, Pérez-Calatayud J. A practical guide to quality control of brachytherapy equipment. ESTRO, Brussels 2004; 151-161.
4. Nath R, Anderson LL, Meli JA et al. Code of practice for brachytherapy physics: Report of the AAPM Radiation Therapy Committee Task Group No. 56. *Med Phys* 1997; 24: 1557-1598.
5. Rivard MJ. Brachytherapy dosimetry parameters calculated for a ^{131}Cs source. *Med Phys* 2007; 34: 754-762.
6. Tailor R, Ibbott G, Lampe S et al. Dosimetry characterization of a ^{131}Cs brachytherapy source by thermoluminescent dosimetry in liquid water. *Med Phys* 2008; 35: 5861-5868.
7. Mason D, Battista J, Barnett R et al. Ytterbium-169: Calculated physical properties of a new radiation source for brachytherapy. *Med Phys* 1992; 19: 695-703.
8. Medich DC, Tries MA, Munro JJ 2nd. Monte Carlo characterization of an ytterbium-169 high dose rate brachytherapy source with analysis of statistical uncertainty. *Med Phys* 2006; 33: 163-172.
9. Ballester F, Granero D, Perez-Calatayud J et al. Study of encapsulated ^{170}Tm sources for their potential use in brachytherapy. *Med Phys* 2012; 37: 1629-1637.
10. Enger SA, D´Amours M, Beaulieu L. Modeling a hypothetical ^{170}Tm source for brachytherapy applications. *Med Phys* 2011; 38: 5307-5310.
11. Enger SA, Lundqvist H, D'Amours M et al. Exploring ^{57}Co as a new isotope for brachytherapy applications. *Med Phys* 2012; 39: 2342-2345.
12. Enger SA, Fisher DR, Flynn RT. Gadolinium-153 as a brachytherapy isotope. *Phys Med Biol* 2013; 58: 957-964.
13. Stenzel Ch, Schroer Ch, Lengeler B et al. Radioisotope Rh-101 as X-ray source for instruments on space missions. http://citeseerx.ist.psu.edu/viewdoc/summary?doi=10.1.1.296.3653, Accessed July 19, 2014.
14. Granero D, Pérez-Calatayud J, Casal E et al. A dosimetric study on the Ir-192 high dose rate Flexisource. *Med Phys* 2006; 33: 4578-4582.
15. http://nucleardata.nuclear.lu.se/toi/nuclide.asp?iZA=450101, Accessed July 19, 2014
16. Waters LS, MCNPX User's Manual, Version 2.4.0., Report LA-CP-02-408 2000, Los Alamos National Laboratory.
17. Ghorbani M. Personal communication with Mahdi Ghorbani, 2015.
18. Rivard MJ, Melhus CS, Wazer DE et al. Dosimetric characterization of round HDR ^{192}Ir accuboost applicators for breast brachytherapy. *Med Phys* 2009; 36: 5027-5032.
19. Lymperopoulou G, Papagiannis P, Sakelliou L et al. A dosimetric comparison of ^{169}Yb versus ^{192}Ir for HDR prostate brachytherapy. *Med Phys* 2005; 32: 3832-3842.
20. Smith DS, Stabin MG. Exposure rate constants and lead shielding values for over, 1100 radionuclides. *Health Phys* 2012; 102: 271-291.
21. Lymperopoulou G, Papagiannis P, Angelopoulos A et al. A dosimetric comparison of ^{169}Yb and ^{192}Ir for HDR brachytherapy of the breast, accounting for the effect of finite patient dimensions and tissue inhomogeneities. *Med Phys* 2006; 33: 4583-4589.
22. Rasulbaev M. Isotopes for fundamental research ^{83m}Kr for KATRIN and ^{101}Rh and ^{109}Cd for XRD studies on planets. PhD Thesis, http://tdpac.hiskp.uni-bonn.de/doktorarbeiten/Doktorarbeit-Maqsud-Rasulbayev-2010.pdf, Accessed 31 October 2014, University of Bonn, 2010.
23. Popkiewicz M, Osuch S, Szeflinski Z et al. Neutron emission from ^{101}Rh produced via ^{12}C+^{89}Y reaction at 49.5 MeV. *Acta Physica Polonica B* 1998; 29: 447-450.
24. Adams QE, Xu J, Breitbach EK et al. Interstitial rotating shield brachytherapy for prostate cancer. *Med Phys* 2014; 41: 051703.
25. Chen Z, Nath R. A systematic evaluation of the dose-rate constant determined by photon spectrometry for twenty-one different models of low energy photon-emitting brachytherapy sources. *Phys Med Biol* 2010; 55: 6089-6104.
26. Perez-Calatayud J, Ballester F, Das RK et al. Dose calculation for photon-emitting brachytherapy sources with average energy higher than 50 keV: report of the AAPM and ESTRO. *Med Phys* 2012; 39: 2904-2929.
27. http://www.nndc.bnl.gov/chart/decaysearchdirect.jsp?nuc=101RH&unc=nds, Accessed July 19, 2014.
28. Rivard MJ, Granero D, Perez-Calatayud J et al. Influence of photon energy spectra from brachytherapy sources on Monte Carlo simulations of kerma and dose rates in water and air. *Med Phys* 2010; 37: 869-876.
29. Rivard MJ, Venselaar JL, Beaulieu L. The evolution of brachytherapy treatment planning. *Med Phys* 2009; 36: 2136-2153.
30. Papagiannis P, Pantelis E, Karaiskos P. Current state of the art brachytherapy treatment planning dosimetry algorithms. *Br J Radiol* 2014; 87: 20140163.
31. Beaulieu L, Carlsson Tedgren A, Carrier JF et al. Report of the Task Group 186 on model-based dose calculation methods in brachytherapy beyond the TG-43 formalism: current status and recommendations for clinical implementation. *Med Phys* 2012; 39: 6208-6236.